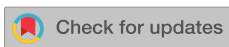


RESEARCH ARTICLE | NOVEMBER 02 2016

Optical spectroscopy study on the photo-response in multiferroic BiFeO₃ ✓

F. Burkert ; J. Kreisel; C. A. Kuntscher



Appl. Phys. Lett. 109, 182903 (2016)

<https://doi.org/10.1063/1.4966548>



Boost Your Optics and Photonics Measurements

Lock-in Amplifier

Zurich Instruments

Find out more

Boxcar Averager

Optical spectroscopy study on the photo-response in multiferroic BiFeO₃

F. Burkert,¹ J. Kreisel,^{2,3} and C. A. Kuntscher^{1,a)}

¹Experimentalphysik 2, Universität Augsburg, D-86159 Augsburg, Germany

²Department Materials Research and Technology, Luxembourg Institute of Science and Technology, 41 Rue du Brill, L-4422 Belvaux, Luxembourg

³Physics and Materials Science Research Unit, University of Luxembourg, 41 Rue du Brill, L-4422 Belvaux, Luxembourg

(Received 16 August 2016; accepted 16 October 2016; published online 2 November 2016)

We investigate the underlying mechanism of the photostriction effect in single-crystalline BiFeO₃ by transmission measurements in the infrared and visible frequency range under continuous illumination with a green laser ($\lambda = 532$ nm). The small photo-induced changes in the transmission spectrum reveal three well-defined absorption features at 1.22 eV, 1.66 eV, and 2.14 eV, which we assign to charge-transfer excitons and in-gap defect states probably related to oxygen vacancies. The intensity of the three absorption features follows a linear dependence on the illumination intensity for an irradiance above 90 W/m². *Published by AIP Publishing.*

[<http://dx.doi.org/10.1063/1.4966548>]

Magnetoelectric multiferroics exhibit both magnetic order and ferroelectricity, coupled with each other, which enables the control of magnetic order via an electric field and the control of the electrical polarization via a magnetic field.^{1–4} Bismuth ferrite BiFeO₃ (BFO) is considered as a prototype magnetoelectric multiferroic due to its ferroelectric and simultaneous antiferromagnetic properties at room temperature and well above.^{5,6} Its piezoelectric properties have also been investigated extensively, suggesting BFO as an interesting lead-free piezoelectric.^{7–9}

The interaction of light with ferroelectrics and multiferroics currently receives a renewed attention notably triggered by reports on large above-bandgap voltages in ferroelectric photovoltaic devices^{10,11} and a wide range of associated properties.^{12,13} In particular, BFO raises interest due to its optical functionality, potentially coupled to its mechanical, magnetic, and electric functionalities. Namely, BFO shows photostriction, i.e., a deformation is induced by irradiation with light, with a very fast response time, which is orders of magnitude faster than that of classical ferroelectrics.^{14–19} The photostriction effect in BFO was first reported by Kundys *et al.*,²⁰ who illuminated a BFO single crystal with a laser ($\lambda = 633$ nm) and an ordinary white light bulb, respectively, and observed a fast, light-induced relative size change of the order of 10^{-5} , depending on the polarization and wavelength of the illumination and external magnetic fields.²¹

The fast photo-induced strain in BFO is attributed to a photovoltaic-based mechanism (rather than to thermal effects) involving the excitation of excitons.^{15,16,22} The spectroscopic evidence for the proposed creation of excitons in BFO is, however, lacking so far due to the limited frequency ranges covered by previous optical studies, probing the optical response in the time-domain.^{16–19}

This work aims at the understanding of excitations under play when BFO is illuminated by light, spectroscopic evidence of excitons is here of particular interest. Earlier optical studies focused on the time-dependent optical response in a

very limited frequency range after a short pump pulse. In contrast to these optical pump-probe experiments, in this letter we probe the optical response in a broad frequency range. We analyze small changes in the transmission spectrum of a thin BFO single crystal during continuous illumination. We observe three photo-induced absorption features close to the absorption edge, which we assign to charge-transfer (CT) excitons and absorption from defect states within the bandgap. Our finding provides further understanding in the electronic processes underlying the photostriction effect in BFO.

The measurements were performed with a Bruker IRScope II infrared microscope, coupled to a Bruker IFS66v/S FTIR spectrometer. For the nearinfrared and visible frequency range (up to 20 000 cm⁻¹) we used an InSb detector, a Si diode, and a Shamrock SR303i CCD spectrograph. A green laser ($\lambda = 532$ nm, $E = 2.3$ eV, $P = 9.1$ mW, cw) was used for illumination of the sample. Several neutral density filters served to reduce the optical output power of the laser. The laser beam was deflected onto the sample by an Al mirror [see Figs. 1(a) and 1(b)]. Due to the grazing incidence,

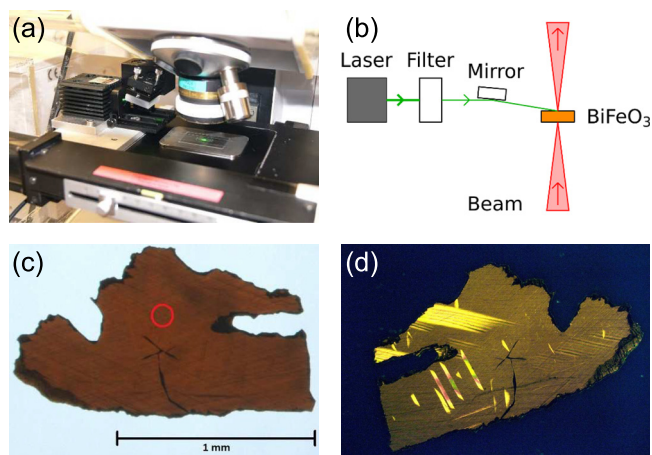


FIG. 1. (a) Photo and (b) sketch of the measurement setup. (c) Photo of the single crystal with the measured position (red circle). (d) Polarized light microscopy image.

^{a)}E-mail: christine.kuntscher@physik.uni-augsburg.de

the laser spot had an elliptical shape at the sample position with an area of $\sim 25 \text{ mm}^2$, which is larger than the studied BFO crystal. The diameter of the circular probing spot is $100 \mu\text{m}$. The choice of the excitation wavelength is based on previous studies showing large deformation and short deformation response time in this case.²¹ The investigated BFO single crystal was grown by flux method (as described elsewhere²³), and polished to a small platelet with a thickness of $\approx 35 \mu\text{m}$ [Fig. 1(c)]. The main contribution to the measured optical response is due to the $[-110]_{pc}$ direction according to polarization-dependent reflectivity measurements of the phonon spectrum.²⁴ Polarized light microscopy revealed the multidomain state of the crystal [Fig. 1(d)]. While such a domain state, especially the domain walls,²⁵ might contribute to the observed signals, we underline that the probing spot on the crystal was kept constant during the measurements so that the observed light-induced changes are representative.

The transmission spectrum of the BFO single crystal and the influence of the illumination on the transmission are depicted in Fig. 2. In the transmission spectrum recorded before illumination and the corresponding absorbance spectrum (see inset of Fig. 2) we observe a steep absorption edge at 2.12 eV, which marks the onset of the charge-transfer excitations across the band gap.^{26,27} Additionally one finds two absorption bands (see inset of Fig. 2) at 1.43 eV and 1.96 eV due to on-site $d-d$ crystal-field excitations ${}^6A_{1g} \rightarrow {}^4T_{1g}$ and ${}^6A_{1g} \rightarrow {}^4T_{2g}$ on the Fe^{3+} ions, respectively.^{26,28-30}

During illumination, one notices a weak decrease in the transmission spectrum in specific frequency ranges (see Fig. 2). These photo-induced spectral changes are better identified in difference spectra (Fig. 3). Therefore, in the following we consider the absolute transmission difference $\Delta T_{abs}(\nu) = I_2(\nu) - I_1(\nu)$, with the intensity $I_1(\nu)$ detected before illuminating the sample (at time t_1) and the intensity $I_2(\nu)$ detected during illumination (at time t_2). To correct ΔT_{abs} for the response function of the particular detector system used, one needs to consider the transmission difference

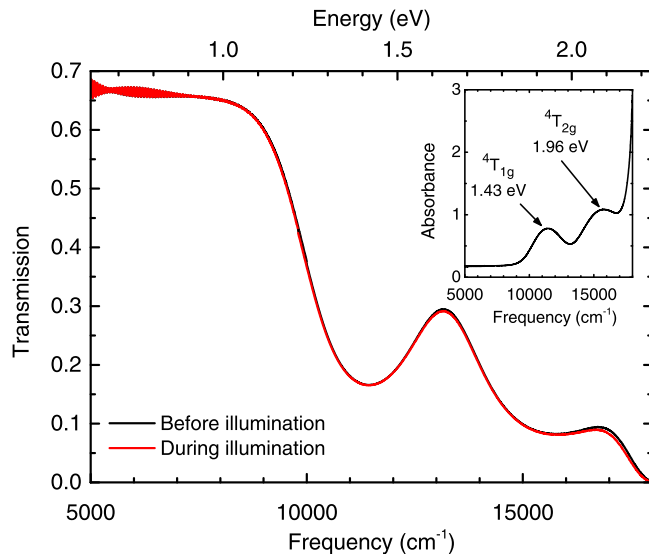


FIG. 2. Comparison of BFO transmission spectra before and during illumination with full laser power. Inset: Corresponding absorbance spectrum [calculated from transmission T according to $A = \log_{10}(1/T)$] without illumination, with the crystal field excitations ${}^4T_{1g}$ and ${}^4T_{2g}$.

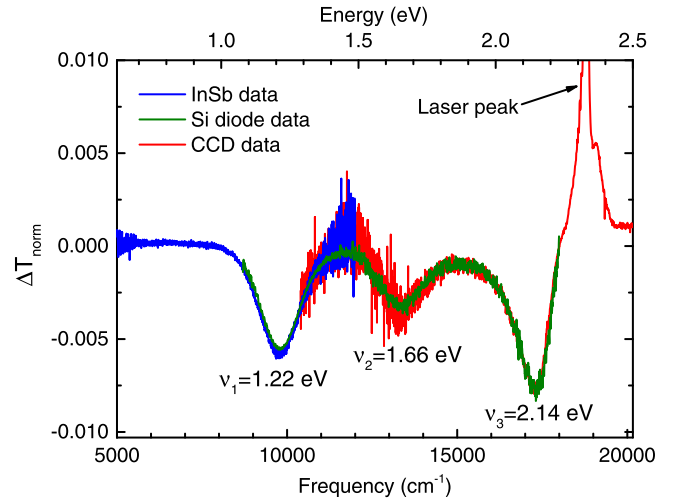


FIG. 3. Normalized transmission difference ΔT_{norm} during illumination with full laser power, revealing three absorption features at frequencies ν_1, ν_2, ν_3 .

ΔT_{norm} normalized by the intensity $I_{ref}(\nu)$ measured for the empty beam path, calculated according to $\Delta T_{norm}(\nu) = \Delta T_{abs}(\nu) / I_{ref}(\nu)$.

The so-obtained normalized transmission difference ΔT_{norm} in Fig. 3 exhibits three weak absorption features with consistent frequencies and intensities for all three detector systems used. The feature frequencies have been determined by fitting with Gaussian functions as $\nu_1 = 9805 \text{ cm}^{-1}$ ($E_1 = 1.22 \text{ eV}$, intensity I_1), $\nu_2 = 13372 \text{ cm}^{-1}$ ($E_2 = 1.66 \text{ eV}$, intensity I_2), and $\nu_3 = 17281 \text{ cm}^{-1}$ ($E_3 = 2.14 \text{ eV}$, intensity I_3), with $I_2 < I_1 < I_3$. The energies of the observed absorption features clearly differ from the energies of the 4T_1 and 4T_2 crystal field excitations, the absorption edge energy, and the average band gap energy ($\approx 2.74 \text{ eV}$) in BFO.²⁹⁻³² We did not detect any further features above 20000 cm^{-1} (not shown).

We also observe a dependence of the intensity of the three absorption features on the intensity of the illumination. A reduction of the laser intensity by neutral density filters leads to a decrease of the feature intensity (see Fig. 4). For a quantitative analysis, we determined the intensities of the

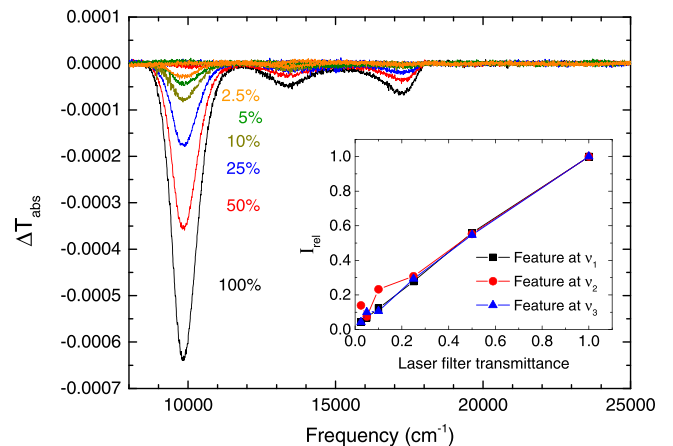


FIG. 4. Absolute transmission difference ΔT_{abs} measured with the Si diode for various laser illumination intensities (in %). Inset: Relative intensity I_{rel} of each feature, normalized to its maximum value measured for the full laser intensity, as a function of laser filter transmittance.

three features for various laser intensities by fitting with Gaussian functions. For each feature we then calculated the relative intensity I_{rel} normalized to its maximum value measured for the full laser intensity. The inset of Fig. 4 shows I_{rel} for each feature as a function of laser filter transmittance. The relation between illumination intensity and feature intensity is linear, except for the slight deviations caused by a low signal-to-noise ratio (SNR) for weak illumination intensities.

We will now discuss our finding of three photo-induced absorption features regarding the photostriction effect in BFO. The phenomenon of photostriction in ferroelectrics is generally explained in terms of a combination of photovoltaic and inverse piezoelectric effects.^{12,20,33} The incident radiation creates electron-hole pairs, which are separated by the internal electric field caused by the ferroelectric polarization, leading to the photovoltaic effect.^{11,34,35} The photovoltaic voltage creates a strain (inverse piezoelectric effect), which leads to photostriction. This picture, however, cannot account for the instantaneous character of the photoinduced stress, demonstrated by several time-resolved experiments, and a consensus about the microscopic explanation of the photostriction effect in BFO is lacking so far.^{15,16,22} Most recent studies propose the excitation of charge-neutral excitons,^{18,36} which are either self-trapped, leading to an instantaneous stress due to the inverse piezoelectric effect,¹⁵ or diffuse to the surface or interface, where they dissociate causing the screening of the depolarization field, which leads to a structural piezoelectric response.²² Despite their discrepancies regarding the detailed microscopic mechanism, recent studies agree in that an photovoltaic-based, non-thermal mechanism is underlying the photostriction effect in BFO. These proposed photo-generated excitons created in BFO were not observed spectroscopically up to now, mainly due to the limited frequency range of previous optical measurements.^{16–19}

In classical semiconductors, the exciton states appear in the band structure as electron-hole bound states below the bottom of the conduction band.³⁷ There are only a few studies on excitonic excitations in ferroelectrics. Excitons in ferroelectrics constitute a particular case, since the environment is highly polarizable with a dielectric constant $\epsilon_1 \gg 1$, which results in very weak electron-hole bonding.³⁸ Additionally, electron correlation effects could play a role, like in BFO. Perovskite-type ferroelectrics are furthermore expected to show covalence effects with charge transfer, leading to the formation of self-trapped $p-d$ charge-transfer (CT) excitons resulting in the appearance of in-gap bands.³⁶ Several recent studies stress the importance of (either localized or diffusing) excitons^{15,22} for the photostriction effect in BFO. Our finding of absorption features close to the absorption edge supports a mechanism involving excitons. Furthermore, it was suggested that vibronic interactions of the CT excitons with the lattice, e.g., with soft lattice transverse optical modes, are relevant, leading to the formation of so-called charge-transfer vibronic excitons (CTVEs) in ABO_3 ferroelectric perovskites.^{39,40} The lattice distortion caused by the CTVEs is predicted to induce local in-gap energy levels. Within this scenario, our observation of three absorption features hints for vibronic interactions involving various vibrational modes.

Absorption from in-gap defect states due to oxygen vacancies could also lead to excitations in this energy range, as was shown experimentally (at ≈ 2.4 eV)^{41,42} and predicted theoretically (at 2.2 eV).⁴³ The absorption feature observed in our data at $E_3 = 2.14$ eV could indeed be attributed to such defect states. For the two lower-energy features, an assignment in terms of excitons is, however, the most likely interpretation. Future studies of the photo-response in single-domain crystals or focusing on the temperature and polarization dependence could provide further important insight.

In conclusion, we have studied the transmission spectrum in the infrared and visible frequency range on single-crystalline BFO under continuous illumination. We observe three photo-induced absorption features below the absorption edge, whose intensity shows a linear dependence on the illumination intensity. The absorption features are assigned to excitonic excitations, like $p-d$ charge transfer excitons or charge-transfer vibronic excitons, and absorption from in-gap defect states probably related to oxygen vacancies. Our findings confirm the relevance of excitons for the photostriction effect in BFO.

This work was financially supported by the Deutsche Forschungsgemeinschaft (DFG) through Grant No. KU 1432/9-1. J.K. acknowledges support from the National Research Fund, Luxembourg through a Pearl grant (Grant No. FNR/P12/4853155).

- ¹M. Fiebig, *J. Phys. D: Appl. Phys.* **38**, R123 (2005).
- ²M. Fiebig, *Phase Trans.* **79**, 947 (2006).
- ³R. Ramesh and N. A. Spaldin, *Nat. Mater.* **6**, 21 (2007).
- ⁴W. Eerenstein, N. D. Mathur, and J. F. Scott, *Nature* **442**, 759 (2006).
- ⁵G. Catalan and J. F. Scott, *Adv. Mater.* **21**, 2463 (2009).
- ⁶G. A. Smolenskii, V. A. Isupov, A. I. Agranovskaya, and N. N. Krainik, *Sov. Phys. Solid State* **2**, 2651 (1961).
- ⁷J. Wang, *Science* **299**, 1719 (2003).
- ⁸D. Lebeugle, D. Colson, A. Forget, M. Viret, P. Bonville, J. F. Marucco, and S. Fusil, *Phys. Rev. B* **76**, 024116 (2007).
- ⁹S. Fujino, M. Murakami, V. Anbusathaiah, S.-H. Lim, V. Nagarajan, C. J. Fennie, M. Wuttig, L. Salamanca-Riba, and I. Takeuchi, *Appl. Phys. Lett.* **92**, 202904 (2008).
- ¹⁰S. Y. Yang, L. W. Martin, S. J. Byrnes, T. E. Conry, S. R. Basu, D. Parani, L. Reichertz, J. Ihlefeld, C. Adamo, A. Melville, Y.-H. Chu, C.-H. Yang, J. L. Musfeldt, D. G. Schlom, J. W. Ager, and R. Ramesh, *Appl. Phys. Lett.* **95**, 062909 (2009).
- ¹¹S. Y. Yang, J. Seidel, S. J. Byrnes, P. Shafer, C.-H. Yang, M. D. Rossell, P. Yu, Y.-H. Chu, J. F. Scott, J. W. Ager, L. W. Martin, and R. Ramesh, *Nat. Nanotechnol.* **5**, 143 (2010).
- ¹²J. Kreisel, M. Alexe, and P. A. Thomas, *Nat. Mater.* **11**, 260 (2012).
- ¹³C. Paillard, X. Bai, I. C. Infante, M. Guennou, G. Geneste, M. Alexe, J. Kreisel, and B. Dkhil, *Adv. Mater.* **28**, 5153 (2016).
- ¹⁴B. Kundys, *Appl. Phys. Rev.* **2**, 11301 (2015).
- ¹⁵D. Schick, M. Herzog, H. Wen, P. Chen, C. Adamo, P. Gaal, D. G. Schlom, P. G. Evans, Y. Li, and M. Bargheer, *Phys. Rev. Lett.* **112**, 097602 (2014).
- ¹⁶H. Wen, P. Chen, M. P. Cosgriff, D. A. Walko, J. H. Lee, C. Adamo, R. D. Schaller, J. F. Ihlefeld, E. M. Dufresne, D. G. Schlom, P. G. Evans, J. W. Freeland, and Y. Li, *Phys. Rev. Lett.* **110**, 037601 (2013).
- ¹⁷L. Y. Chen, J. C. Yang, C. W. Luo, C. W. Laing, K. H. Wu, J.-Y. Lin, T. M. Uen, J. Y. Juang, Y. H. Chu, and T. Kobayashi, *Appl. Phys. Lett.* **101**, 41902 (2012).
- ¹⁸Y. M. Sheu, S. A. Trugman, Y.-S. Park, S. Lee, H. T. Yi, S.-W. Cheong, Q. X. Jia, and A. J. T. R. P. Prasankumar, *Appl. Phys. Lett.* **100**, 242904 (2012).
- ¹⁹P. Ruello, T. Pezeril, S. Avanesyan, G. Vaudel, V. Gusev, I. C. Infante, and B. Dkhil, *Appl. Phys. Lett.* **100**, 212906 (2012).
- ²⁰B. Kundys, M. Viret, D. Colson, and D. O. Kundys, *Nat. Mater.* **9**, 803 (2010).
- ²¹B. Kundys, M. Viret, C. Meny, V. Da Costa, D. Colson, and B. Doudin, *Phys. Rev. B* **85**, 092301 (2012).

- ²²Y. Li, C. Adamo, P. Chen, P. G. Evans, S. M. Nakhmanson, W. Parker, C. E. Rowland, R. D. Schaller, D. G. Schlom, D. A. Walko, H. Wen, and Q. Zhang, *Sci. Rep.* **5**, 16650 (2015).
- ²³R. Haumont, R. Saint-Martin, and C. Byl, *Phase Trans.* **81**, 881 (2008).
- ²⁴R. Haumont, P. Bouvier, A. Pashkin, K. Rabia, S. Frank, B. Dkhil, W. Crichton, C. Kuntscher, and J. Kreisel, *Phys. Rev. B* **79**, 184110 (2009).
- ²⁵J. Seidel, D. Fu, S.-Y. Yang, E. Alarcon-Llado, J. Wu, R. Ramesh, and J. W. Ager III, *Phys. Rev. Lett.* **107**, 126805 (2011).
- ²⁶B. Ramachandran, A. Dixit, R. Naik, G. Lawes, and M. S. R. Rao, *Phys. Rev. B* **82**, 012102 (2010).
- ²⁷J. B. Neaton, C. Ederer, U. V. Waghmare, N. A. Spaldin, and K. M. Rabe, *Phys. Rev. B* **71**, 014113 (2005).
- ²⁸S. Gómez-Salces, F. Aguado, F. Rodríguez, R. Valiente, J. González, R. Haumont, and J. Kreisel, *Phys. Rev. B* **85**, 144109 (2012).
- ²⁹X. S. Xu, T. Brinzari, S. Lee, Y. Chu, L. Martin, A. Kumar, S. McGill, R. Rai, R. Ramesh, V. Gopalan, S. Cheong, and J. Musfeldt, *Phys. Rev. B* **79**, 134425 (2009).
- ³⁰A. Kumar, R. C. Rai, N. J. Podraza, S. Denev, M. Ramirez, Y.-H. Chu, L. W. Martin, J. Ihlefeld, T. Heeg, J. Schubert, D. G. Schlom, J. Orenstein, R. Ramesh, R. W. Collins, J. L. Musfeldt, and V. Gopalan, *Appl. Phys. Lett.* **92**, 121915 (2008).
- ³¹J.-P. Xu, R.-J. Zhang, Z.-H. Chen, Z.-Y. Wang, F. Zhang, X. Yu, A.-Q. Jiang, Y.-X. Zheng, S.-Y. Wang, and L.-Y. Chen, *Nanoscale Res. Lett.* **9**, 188 (2014).
- ³²J. F. Ihlefeld, N. J. Podraza, Z. K. Liu, R. C. Rai, X. Xu, T. Heeg, Y. B. Chen, J. Li, R. W. Collins, J. L. Musfeldt, X. Q. Pan, J. Schubert, R. Ramesh, and D. G. Schlom, *Appl. Phys. Lett.* **92**, 142908 (2008).
- ³³P. Poosanaas, A. Dogan, S. Thakoor, and K. Uchino, *J. Appl. Phys.* **84**, 1508 (1998).
- ³⁴T. Choi, S. Lee, Y. J. Choi, V. Kiryukhin, and S.-W. Cheong, *Science* **324**, 63 (2009).
- ³⁵A. Bhatnagar, A. R. Chaudhuri, Y. H. Kim, D. Hesse, and M. Alexe, *Nat. Commun.* **4**, 2835 (2013).
- ³⁶R. V. Pisarev, A. S. Moskvina, A. M. Kalashnikova, and T. Rasing, *Phys. Rev. B* **79**, 235128 (2009).
- ³⁷T. Kazimierczuk, D. Fröhlich, S. Scheel, H. Stolz, and M. Bayer, *Nature* **514**, 343 (2014).
- ³⁸V. S. Vikhnin, *Ferroelectrics* **199**, 25 (1997).
- ³⁹R. I. Eglitis, E. A. Kotomin, V. A. Trepakov, S. E. Kapphan, and G. Borstel, *J. Phys.: Condens. Matter* **14**, L647 (2002).
- ⁴⁰V. S. Vikhnin, R. I. Eglitis, S. E. Kapphan, G. Borstel, and E. A. Kotomin, *Phys. Rev. B* **65**, 104304 (2002).
- ⁴¹A. J. Hauser, J. Zhang, L. Mier, R. A. Ricciardo, P. M. Woodward, T. L. Gustafson, L. J. Brillson, and F. Y. Yang, *Appl. Phys. Lett.* **92**, 222901 (2008).
- ⁴²M. C. Weber, M. Guennou, C. Toulouse, M. Cazayous, Y. Gillet, X. Gonze, and J. Kreisel, *Phys. Rev. B* **93**, 125204 (2016).
- ⁴³S. J. Clark and J. Robertson, *Appl. Phys. Lett.* **94**, 022902 (2009).